Physical and numerical modelling of the response of slopes under different rainfalls, inclinations and vegetation conditions

Diana Salciarini,* Renato Morbidelli,* Elisabetta Cattoni,** Evelina Volpe***

Summary

We present the results of an experimental and numerical study focused at quantifying the effect of different crucial factors in slope evolution, such as: rainfalls, inclinations and vegetation conditions. To this aim a small-scale slope was constructed in the laboratory and an experimental program was design to understand the slope response under the following conditions: a) different inclinations, obtained through a system of hydraulic pistons; b) different rainfall conditions (in intensity and duration), obtained through an artificial rain simulator; c) presence / absence of a vegetated cover. The first set of tests allowed defining a trend for the percentage of rainfall infiltration within the slope as a function of the steepness. The second set of tests allowed observing the bare slope behaviour at failure; while the third set demonstrated the beneficial effect of a grass carpet. All the laboratory experiments were integrated by numerical simulations, using the SEEP/w FE code for transient infiltration analyses and the SLOPE/w code for stability analyses. The back-analyses, based on the classical Equilibrium Limit Methods, allowed estimating the enhanched shear strength provided by the presence of the roots, relevant in the practice for remedial works based on Soil Bio-Engineering.

1. Introduction

Recently, many efforts have been done to deepened the knowledge on the response of a slope under climatic actions (see among others, *e.g.*, Picarelli 2007; Cascini *et al.*, 2010; Cascini *et al.*, 2011; Cotecchia *et al.*, 2014; Salciarini *et al.*, 2020a; Volpe *et al.*, 2021). As well known, the climatic variables, mainly rainfalls, affect the stress-strain condition within the slope and, thus, its stability conditions in a variable manner depending on the water infiltration process, which is ruled by many factors. For example, slope inclination (geometric aspect), soil permeability (hydraulic aspect), and presence of vegetation have a predominant role in determine the inlet flow and outflow at the slope top boundary, that, in turn, produce variations in terms of: void ratio, e; suction u; degree of saturation, S_r, and hence, distribution of the pore water pressures in the seepage domain (see, *e.g.*, Cammeraat *et al.*, 2005; Cotecchia *et al.*, 2014; Rotisciani *et al.*, 2020, 2021).

* Department of Civil and Environmental Engineering – Università degli Studi di Perugia, Italy
** University eCampus, Novedrate (CO), Italy
*** National Research Council of Italy, Research Institute for Geo-Hydrological Protection, Italy

Among the listed factors influencing the infiltration process, which has a fundamental role in the transformation of inflows-outflows, the slope gradient effect is a still unsolved problem [Morbidelli *et al.*, 2019]. The surface water velocity, negligible over horizontal soil surface [Smith *et al.*, 1978; Corradini *et al.*, 1997; Corradini *et al.*, 2011], has an important role in seepage problems within inclined slopes, as demonstrated by literature contributions devoted to mathematical modeling and laboratory tests [Beven, 2002; Morbidelli *et al.*, 2018; Morbidelli *et al.*, 2015].

Another important variable that still deserves more investigation is the presence of the vegetation over the soil cover. This can affect slope stability in two ways: changing in the soil moisture regime and contribution to soil strength exerted by the roots [Liu *et al.*, 2016; Fay L. *et al.*, 2012; Khalilzad *et al.*, 2014]. In general, it is found that vegetation improves the mechanical and hydraulic characteristics of the soil reducing the soil vulnerability to erosion and landsliding [Bordoloi *et al.*, 2020; Zayadi *et al.*, 2020]. In the last decade, to contrast the significant increase in shallow landslides [Salciarini *et al.*, 2015, 2017, 2019; Haque *et al.*, 2019; Gariano *et al.*, 2020] a new branch of slope engineering has grown up, based on the use of vegetation to reduce the hydrogeological hazard [Lammeranner *et al.*, 2005; Wu, 2006; Wu *et al.*, 2015] and

 dx.doi.org/10.19199/2022.1.0557-1405.047

named "Soil Bio-Engineering (SBE)". This is a discipline including techniques of re-naturalization; anti-erosion and stabilization of shallow covers; and, as defined in [MORGAN *et al.*, 2003], it involves the use of all plant species, whether represented by a single plant or a set of plants, considered as an engineering building material. To rationally apply the SBE methods for landslide hazard mitigation, it is important to fully understand the effects due to the presence and role of vegetation on slope. First, vegetation dissipates most of the kinetic energy of raindrops, weakening the erosion action. The degree of interception depends on the density of the leaves and the size of the plant. From the geomechanical and stabilization point of view, the most important effect is the mechanical reinforcement exerted by the roots, analysed by different authors (see, *e.g.*, in WALDRON, 1977; WU *et al.*, 1979; WU, 2006; OPERSTEIN *et al.*, 2000; STOKES *et al.*, 2009; WU *et al.*, 2013). This consists in an increase in the shear strength in the portion of vegetated soil, which is typically included in the Mohr–Coulomb failure criterion as additional soil cohesion [CAZZUFFI *et al.*, 2006; NORRIS *et al.*, 2006; WU *et al.*, 2015]. Examples of BSE practical applications against landslide hazard are described in, *e.g.*, FLORINETH *et al.* [2002]; CALCATERRA *et al.* [2004]; PETRONE and PETRI [2009]; ZAROTTI *et al.* [2014]; SALCIARINI *et al.* [2020b] for different climatic areas in the world.

In this paper we present the results of a study that examines the response of a slope considering all the variables listed so far: climatic factors (rainfalls); slope inclination; and presence/absence of a vegetated cover. To this aim, laboratory experiments were designed to investigate the evolution of slopes under such different environmental/boundary conditions. The system consists of a small-scale slope, an artificial rain simulator designed to provide steady and uniform rainfall, placed directly above the slope, and a high-resolution camera to record the behaviour of the slope. Such equipment has made it possible to observe the slope evolution (in terms of infiltration mechanism and stability condition) when characterized by: *i*) different inclinations of the topographical surface; *ii*) different rainfall conditions typical of the Mediterranean climatic area; and, *iii*) different exposed surface (bare/vegetated).

The experimental results have been then reproduced by numerical simulations, both considering the infiltration process using the SEEP/w FE code, and the improvement in slope stability due to the vegetation using the SLOPE/w FE code. In particular, the slope stability analyses, comparing the case of bare and vegetated soil, have been aimed at assessing the additional shear resistance introduced by the presence of the roots.

The paper is organized as follows: after this introduction, the description of the experimental setup for the laboratory tests is given in section 2. In section 3 the three groups of testing are presented. section 4 is dedicated to the numerical modelling of the infiltration and the stability analyses, while in section 5 the obtained results are shown and discussed. Finally, in section 6 some concluding remarks are given.

2. Experimental setup

Laboratory experiments have been designed to investigate the evolution of slopes under different rainfalls, inclinations, and (bare or vegetated) surfaces. A small-scale slope has been implemented and rainfall is applied through a rainfall simulator device, designed to provide steady and uniform rainfall and placed directly above the slope. Figure 1 shows a picture of the system prepared for the experimental campaign, while figure 2 shows two sketches of the equipment (3D and lateral view) to provide details on the positions of the collectors, artificial rainfall simulator and tipping bucket sensors.

The basic components of the experimental setting consist of: *i*) a hydraulic network and hydrologic measuring equipment to control the inflow/outflow process and measure the surficial/sub-surficial flow rate; *ii*) supply and distribution systems; *iii*) rain simulator; *iv*) artificial slope; *v*) data acquisition system; *vi*) high-resolution camera to record the slope stability evolution.

The hydraulic network connects the accumulation reservoir and rain simulator; it allows deriving, from the air tank (item A in Fig. 3) small flow rates. Starting from the storage tank (VDA in Fig. 3) the distribution system is composed of 3 submerged



Fig. 1 – Laboratory test equipment: small-scale slope and rainfall simulator.
Fig. 1 – Attrezzatura di laboratorio: cassone per riprodurre il pendio a piccola scala e simulatore artificiale di pioggia.

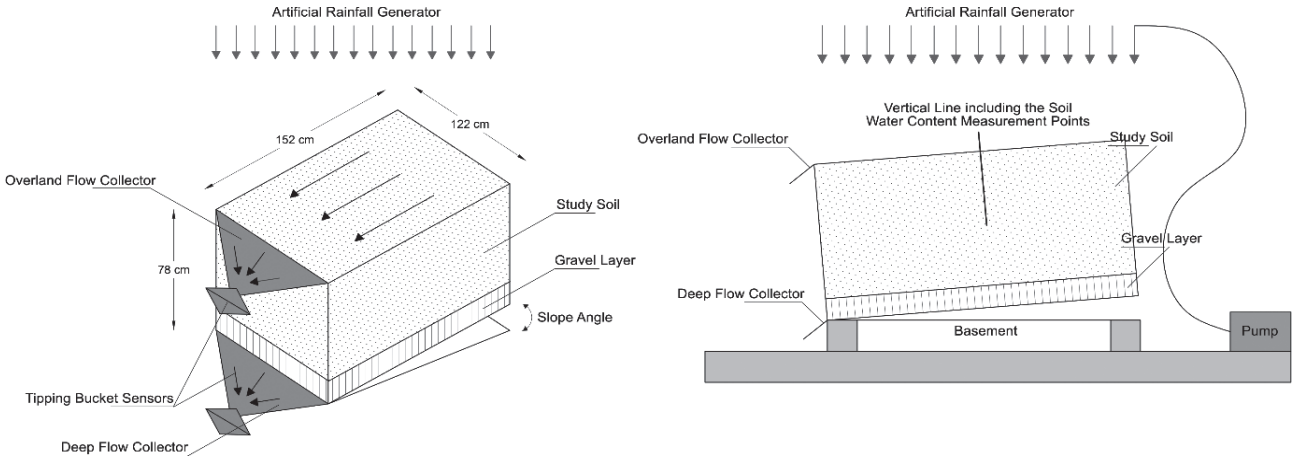

Fig. 2 – Sketch of the laboratory test equipment: small-scale slope and rainfall simulator.
Fig. 2 – Schema dell'attrezzatura di laboratorio: cassone per riprodurre il pendio a piccola scala e simulatore di pioggia.

pumps; P3 supplies the rainfall simulator (SM in Fig. 3). VDA and SM are connected by a pipeline; the ball valve V2 allows to stop the flow and V3 is used to provide the flow regulation. The filter (F) purifies the water and avoids the nozzle obstruction.

The sprayer, which transforms the flow coming from the supply network into artificial rainfall, ends with 2 *Fulljet* nozzles that produce a full cone jet with a circular section and spray angles between 120° and 125°. The jet, uniform on the area to be wet, reproduces drops similar to natural rains.

The small-scale slope (item P, in Fig. 3) is made of a galvanized steel box with dimensions of 152×122×78 cm, with a plexiglass side wall for the complete observation of the mechanical phenomena that occur in the artificial slope. At the front wall two collectors with balancing-tank gauges guarantee the drainage and measure of the surficial and deep flow. Such gauges generate an electrical impulse at the overturning of the balancing tanks recorded by 2 measurement stations linked respectively to the surface and deep flows (S1 and S2, in Fig. 3).

The base of the box is connected to a system of hinges and hydraulic pistons able to incline the box reproducing different inclinations of the slope.

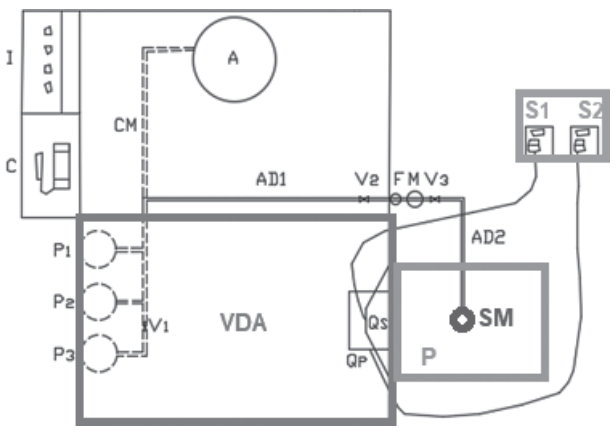

Fig. 3 – Sketch of the hydraulic network and laboratory testing equipment.
Fig. 3 – Schema del circuito idraulico e dei collegamenti alle attrezzature di laboratorio.

2.1. The small-scale slope

Figure 4 shows a sketch of the experimental box used to simulate the small-scale slope in laboratory and table 1 summarizes the geometric measures. The box can have different inclinations, controlled by the hydraulic pistons at the basis. Here the small-scale slope is represented in its final configuration used for the stability analyses, with the maximum inclination of 30° and a local modification of the ge-

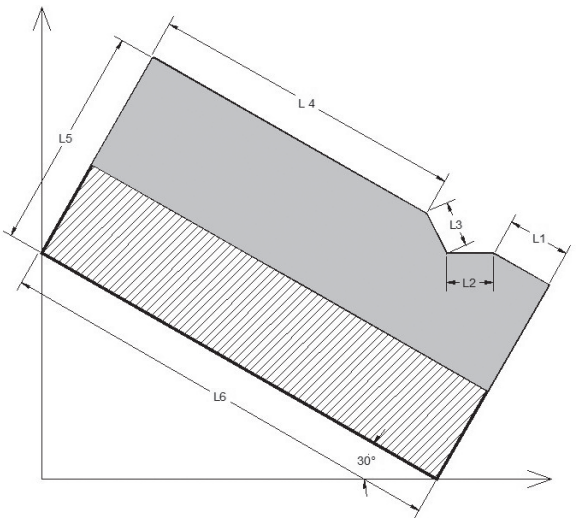

Fig. 4 – Sketch of the experimental box used to simulate the small-scale slope.
Fig. 4 – Schema della geometria del cassone impiegato per simulare il pendio.

Tab. I – Dimensions of the different geometric elements of the box.
Tab. I – Sintesi delle dimensioni geometriche del cassone.

L1	L2	L3	L4	L5	L6	Unit
0.20	0.15	0.15	1.05	0.75	1.5	(m)

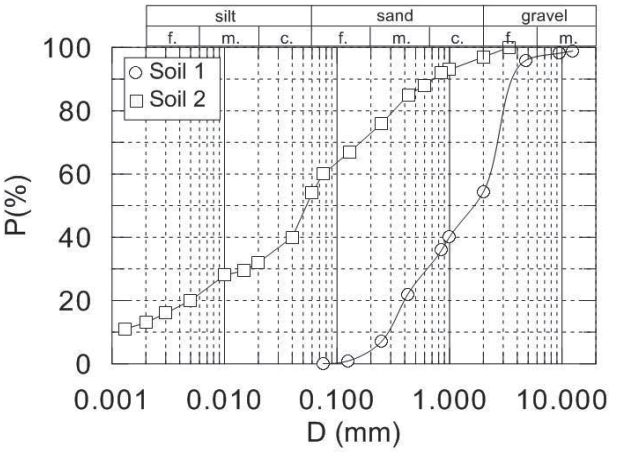

Fig. 5 – Grain size distribution of Soil 1 and Soil 2.
Fig. 5 – Curve granulometriche dei terreni 1 e 2.

ometry in the low part of the topographical surface, to simulate the presence of an excavation work.

The box is filled with two layers of soil: the upper layer, of 40 cm thickness, is a gravelly sand (hereafter named Soil 1); the lower layer, of about 35 cm thickness, is a silty sand (hereafter named Soil 2). The soil grain size distributions are shown in figure 5.

Saturated hydraulic conductivity of the upper soil layer was experimentally assessed by previous works by MORBIDELLI *et al.* [2015] and is equal to K_s = 4.6e-6 m/s. Shear strength values for Soil 1 have been obtained from simple direct shear tests (DS) on soil samples collected from the box in the upper layer, which revealed an initial void index equal to 0.8. The lower layer is not involved in failure mechanism and the shear strength has not investigated. The results of the DS test are shown in figure 6 in terms of shear stress τ *vs* horizontal displacements Δx (Fig. 6a) and vertical displacements Δy *vs* horizontal displacements Δx (Fig. 6b). The soil samples have been consolidated at different values of vertical effective stress σ_v = 100 – 200 – 400 kPa. The shear strength parameters of Soil 1 (c'≅0 and ϕ=29°) have been determined applying a Mohr–Coulomb failure criterion as shown in figure 6c. The obtained friction angle is at the low boundary of the typical range of mechanical values for gravelly sand soil types, likely attributable to the low density of the soil within the small–scale slope. This is confirmed by the trend of the τ - Δx curves of figure 6b that is consistent with the typical ductile behaviour at failure of poorly dense soils.

3. Experimental tests

Three experimental sessions have been carried out to investigate and compare the slope response under different configurations and environmental conditions. In the first set, a bare slope has been tested under the action of a rainfall simulator device designed to provide steady and uniform rainfall and placed directly above the slope. The rainfall has been kept constant and 4 different tests have been repeated, modifying the inclination of the slope through the system of pistons at the basis of the box. For each test, the steady outflow has been monitored at the surface and at the basis of the box, to investigate hydraulic behaviour.

In the second set, the same bare slope has been tested under the action of different rainfalls, keeping constant the inclination of the box (at the maximum value equal to 30°) and introducing a local variation of the topographical surface. The slope response has been monitored by means of a high-reso-

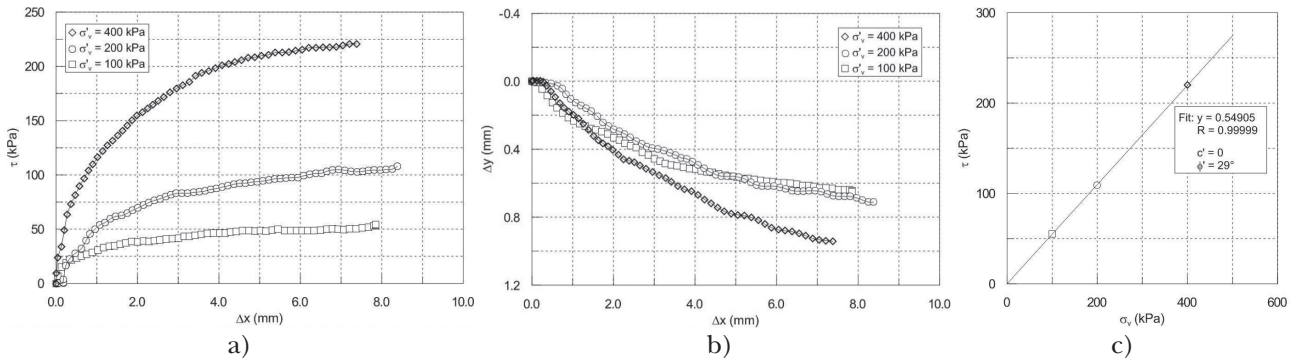

Fig. 6 – Direct shear tests on Soil 1 samples: a) τ - Δx curves; b) Δy - Δx curves; c) failure envelope.
Fig. 6 – Risultati delle prove di taglio diretto sul terreno 1 nei piani: a) τ - Δx; b) Δy - Δx; c) τ - σ, inviluppo di rottura.

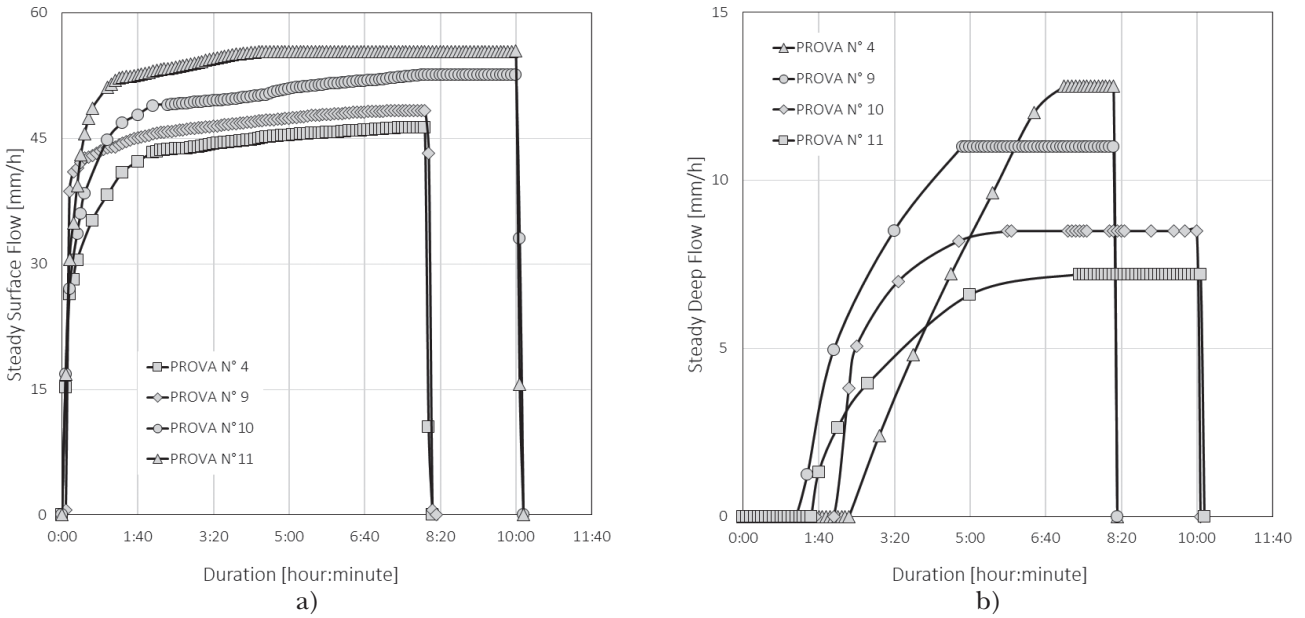

Fig. 7 – Evolution in time of: a) surface flow; and, b) deep flow for different slope gradient.
Fig. 7 – Evoluzione nel tempo del: a) flusso superficiale; b) flusso profondo, al variare della pendenza del cassone.

lution camera, until recording the time of rainfall-induced failure. In this case the downstream wall was modified as an impervious boundary.

Finally, keeping constant the inclination, boundary conditions and rainfall pattern used to bring to failure the bare slope, a vegetated cover has been sown and the tests have been repeated.

3.1. Effect of the inclination on the infiltration process

Theoretical models for infiltration problems often neglect the contribution of surface flow [SMITH *et al.*, 1978; CORRADINI *et al.*, 1997; CORRADINI *et al.*, 2011]. This hypothesis, valid for near horizontal soil surfaces, is not completely appropriate for steep slopes [BEVEN, 2002; MORBIDELLI *et al.*, 2018; MORBIDELLI *et al.*, 2015].

To quantify the effect of the steepness on the surface flow (S_F), experimental tests have been carried out considering slope inclinations (α) in a range of 10°- 26° under the action of a heavy rainfall (about 60 mm/h) obtained by the rain simulator described in section 2. Before the beginning of each tests, a low-rate rainfall was applied in order to have high soil water content at any depth; the surface water content was kept sufficiently high in the time period between two successive tests to avoid creeping.

Surface and deep flows (S_F and D_F, respectively) were monitored by calibrated sensors based on a tipping-bucket mechanism at the downstream wall of the box (see Sect. 2 for description). Figure 7 shows the evolution of the surface and deep flow in time, for the 4 tests performed at different inclinations, while table II summarizes the obtained results for the tests conducted in terms of percentage of surface flow (S_F) and deep flow (D_F) with respect to the average rainfall rate.

The results in figure 7 and table I for the studied soil show that as the steep slope inclination increases, the steady surface flow increases and, consistently, the steady deep flow decreases. For the soil considered, with the maximum inclination investigated of 26°, the surface flow reaches the 88.5% of the rainfall rate, and the related deep flow is 11.5%. The relation between S_F, D_F and α, under the same rainfall intensity has a trend about linear, as shown in figure 8).

3.2. Effect of rainfalls on a bare slope

The second group of tests on the artificial slope has been dedicated to the observation of the slope response in terms of stability under different rainfalls. The box has been brought to an inclination of 30°, since from the previous set of tests (see Sect. 3.1) no failure was observed. Also, in the lower part of the small-scale slope, a cut simulating an excavation work has been realized. The steepness of the cut is 60°, as shown in figure 4.

Two rainfall events produced by the rain simulators have been considered, over the small-scale slope:
– a low-rate rainfall, with I=15 mm/h
– a high-rate rainfall, with I=60 mm/h

The first rainfall (I = 15 mm/h) has been prolonged for a duration of 8 hours, and this has not been able to produce any failure mechanism

Tab. II – Percentage of steady surface and deep flow in relation to average rainfall rate.
Tab. II – Percentuale di flusso superficiale e profondo registrato, rispetto al valor medio di pioggia applicata.

Test n.	Inclination (°)	Average rainfall rate (mm/h)	S_F (%)	D_F (%)
1	10	59.10	78.34	21.66
2	17	59.36	81.46	18.54
3	21	61.10	86.09	13.91
4	26	62.60	88.50	11.50

(Fig. 9a). The second rainfall (I=60 mm/h) has been prolonged for 10 hours and, after 45 minutes, the first failure and movements were recorded by the high-resolution camera on the cut simulating the excavation work in the lower part of the box (Fig. 9b). It is interesting to observe that, despite the quite relevant inclination of the rest of the slope (30°) and the high-rate rainfall, no other landslide mechanism developed in the box. In the upper part of the box is possible to observed only very limited areas of erosion (few millimetres depth).

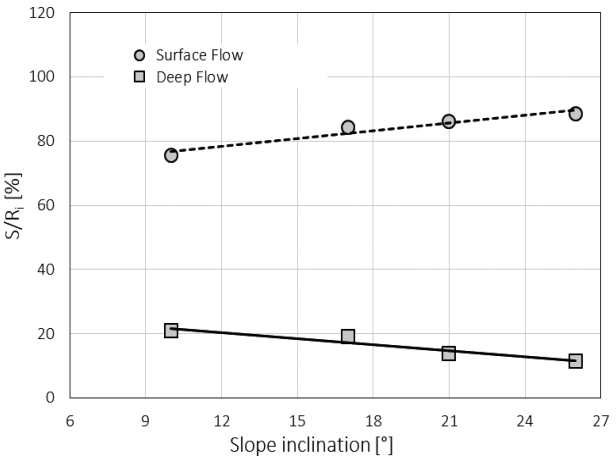

Fig. 8 – Trend of percentage of surface and deep flow rate, with respect to rainfall rate, as a function of slope inclination.
Fig. 8 – Andamento percentuale dei flussi superficiale SF e profondo SD, valutati rispetto alla pioggia applicata, per diversi valori di pendenza del versante.

3.3. Effect of the presence of a vegetated cover

The third group of tests has been performed on the same small-scale slope, with the presence of a vegetated cover, simulating a SBE work. After the failure obtained with the second group of tests (see Sect. 3.2) green grass was sown evenly on the initial topographical profile (reconstructed with the same geometry of that used in the experiments of Sect. 3.2), and the seeds were watered at regular time intervals. After 3 months of root growth, the experimental tests started. Figure 10a shows the vegetated small-scale slope, and figure 10b,c a 6×6 cm vegetated soil sample collected from the upper part of the box, to observe the depth of the roots.

In this phase the experimental research has been focused on the mechanical improvement due to vegetation, and no hydrologic aspects have been monitored. Considering an idealized uniform root architecture, the vegetated slope was subjected to the same rainfall that caused the collapse of the natural slope (I = 60 mm/h). At the end of the experiments (duration of the rainfall d=10 hours) no instabilities nor surficial erosion occurred demonstrating, in empirical manner, the beneficial effect exerted by the roots, whose quantification will be assessed in the next sections.

4. Numerical FE simulations

Despite remedial works based on BSE, characterized by low costs and environmental impact, have

growth in the recent years [PETRONE and PETRI, 2009; FLORINETH *et al.*, 2002; CALCATERRA *et al.*, 2004; ZAROTTI *et al.*, 2014], the quantification of the role of roots in slopes stability is still an open issue (see, *e.g.*, SALCIARINI *et al.*, 2020b). Several authors have summarized results of in situ and laboratory tests, considering different aspects of root reinforcement such as root depths, plant type, growth models etc. [CAZZUFFI *et al.*, 2006; NORRIS *et al.*, 2006]. Vegetation improves the stability conditions of shallow slopes through the hydrological and mechanical effects of plants [LIU *et al.*, 2016; FAY *et al.*, 2012; KHALILZAD *et al.*, 2014]: the hydrological effect results in pore water pressure reduction (and in the decrease of hydraulic conductivity), while the mechanical effects are quantified through an increase of soil shear strength [WU, 2006; OPERSTEIN *et al.*, 2000; STOKES *et al.*, 2009; WU *et al.*, 2013; FENG *et al.*, 2020] in general considered as an additional cohesive effect in the soil (see, *e.g.*, NORRIS *et al.*, 2006; CECCONI *et al.*, 2012; SALCIARINI *et al.*, 2020b).

The experimental tests presented in section 3 provide some qualitative evidences on the slope response; however, to better understand the effect ex-



a) b)

Fig. 9 – Photograms of the small-scale slope: a) after 8 hours of rainfall of I = 15 mm/h; and b) after 45 minutes of rainfall of I = 60 mm/h.

Fig. 9 – Fotogrammi del versante ricostruito in laboratorio durante la sperimentazione: a) dopo 8 ore di pioggia di intensità I = 15 mm/h; e b) dopo 45 minuti di pioggia di intensità I = 60 mm/h.

erted by the vegetation, a 2D model of the small-scale equipment was prepared by means of:

– the SEEP/w code to perform transient FE seepage analyses; and
– the SLOPE/w code to perform slope stability analyses at different times during the transient infiltration process.

The aim of the analyses is to reproduce the infiltration process and the slope failure mechanism observed in the experimental slope in the laboratory, both considering the bare surface and the vegetated surface for the slope, with the goal of quantifying the beneficial effect introduced by the roots.

4.1. Problem setting: geometry and FE model

The model prepared for the seepage analyses represents the experimental box used in the laboratory for the tests described in section 3. The model adopted is constituted of two different soil layers: the upper gravelly sand (Soil 1, in yellow) and the lower silty sand (Soil 2, in green) as shown in figure 11. The soil domain is discretized by means of 449 quadrangles and triangles, four/three-noded elements with two displacement DOFs per node, with a maximum element size of 0.05 m.

The rainfall is applied over the ground surface by means of the boundary conditions of *potential seepage face*, characterized by a constant unit water flux q equal to the rainfall intensity of the e×perimental test. The other three sides of the model, representing the faces of the experimental box, have been considered impermeable by imposing a boundary condition of null water flux ($q = 0$). The initial conditions of transient analyses have been specified imposing the water table at the contact surface between Soil 1 and Soil 2.

Seepage transient analyses have been performed considering the two different rainfall conditions used for the experimentations:

a) rainfall intensity $I = 15$ mm/h and duration $D = 8$ h;
b) rainfall intensity $I = 60$ mm/h and duration $D = 10$ h.

The duration of the rainfall in each transient analysis has been subdivided into 1000 steps with an increment time step size varying from 3 s to 100 s.

Transient analyses have been performed assuming partially saturated behaviour of the soils by means of the SEEP/W code *Saturated/Unsaturated* model. The volumetric water content function and hydraulic conductivity function required as input parameters for transient analyses have been estimated using the predictive method of the code based on the measured grain-size distribution curve. In particular, the SWCC and *K*-function adopted for Soil 1 are those corresponding to a gravel material, while for the Soil 2 have been chosen the hydraulic functions corresponding to a silty-sand material.



Fig. 10 – Vegetated small-scale slope and vegetated soil sample collect from the upper part of the box, to observe the depth of the root.

Fig. 10 – Campioni di terreno con manto erboso, direttamente prelevati dal cassone, al fine di valutare la profondità dell'apparato radicale.

4.2. Simulations program

Preliminary sensitivity analyses have been performed in order to evaluate the influence of hydraulic properties on the seepage results. In particular, for both the rainfall events considered, the effect on the results of saturated volumetric water content θ_s, saturated permeability coefficient K_s and Soil Water Characteristic Curve, has been investigated.

On the base of the preliminary analyses, the hydraulic properties employed on the reference model of the case study are summarized in table III. The aim was to reproduce at better the experimental conditions in the lab. In the FE model a piezometric surface has been placed at 40 cm from the topographical surface. The overlying portion of soil was considered to be in unsaturated conditions. The characteristic curve of this soil volume was reconstructed through the van Genuchten equation. The parameters used for the curve were obtained from library functions starting from the knowledge of the particle size distribution of the material.

For both the rainfall events, slope stability analyses have been conducted at different stages during the transient process. In particular, according to the experimental evidences derived by the small-scale slope in the lab, the slope stability has been evaluated:

– at the end of the first rainfall event (t = 28800 s and I = 15 mm/h) corresponding to the observed stability condition in the laboratory test;
– at t = 2770 s (corresponding to the failure time monitored during the laboratory test) in the case of the rainfall characterized by I = 60 mm/h.

The stability analyses have been carried out using the Morgenstern and Price approach [MORGENSTERN and PRICE, 1965] of the classical Limit Equilibrium Methods, quantifying the safety level of the slope by a single scalar quantity, the Factor of Safety (*FS*), computed as the ratio between the available shear strength and the mobilized shear stress along a potential failure surface.

5. Results

In the following sections 5.1 and 5.2 we present the results of the infiltration analyses for the different rainfalls considered and the relative stability analyses for the bare and vegetated slope under different inclinations (from 17° up to 30°). In the analyses, only the mechanical effect of the reinforcement exerted by the roots has been considered, while the influence of vegetation on the hydraulic properties has been neglected. Although the Authors are aware that the hydrologic effect might be significant in some cases, previous studies demonstrated that the effect of the mechanical reinforcement is prevalent on the slope stability, with respect to the hydraulic one. For example, CHIRICO *et al.* [2013] showed that under a Mediterranean climatic regime, the geo-mechanical effect tends to be more relevant than the soil-hydrological effect during the rainy season; LEUNG *et al.* [2018] showed

Tab. III – Soil hydraulic properties assumed in the seepage analyses.
Tab. III – Proprietà idrauliche del terreno adottate nelle analisi di filtrazione.

Soil	θ_r	θ_s	α	n	K_s
1	0.10	0.37	0.059	1.48	$4.26e^{-6}$
2	0.10	0.33	0.005	1.09	$2.26e^{-6}$

that mechanical reinforcement is effective in shallow depths, where the most root biomass exists. Hydrological reinforcement is much more significant in deeper depths (>1 m), but this effect could vanish due to root-induced increase in hydraulic conductivity.

As discussed in section 2, the adopted shear resistance value for the upper soil layer are derived from a DS test on a purely frictional soil. The numerical tests considering the slope with vegetated soil has been performed to estimate the additional cohesive contribute introduced by the root to bring the slope to a stable condition.

5.1. Case of bare soil

Figure 12 shows the pore water pressure isolines and the water table position at the end of the analysis in the case of the low-rate rainfall event (I = 15 mm/h), and figure 13 shows the results of stability analyses performed at the end of the rainfall event (t = 28800 s). Here, the potentially unstable soil volume is coloured in green, bounded by the

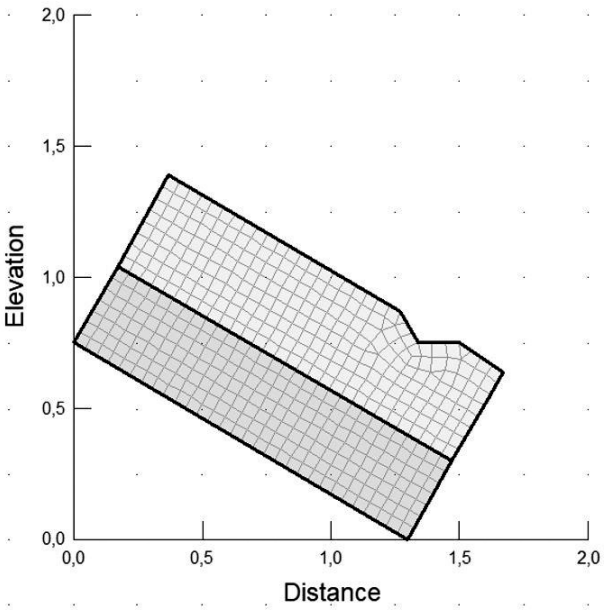

Fig. 11 – Problem geometry and finite element discretization adopted in the FE analyses.
Fig. 11 – Schematizzazione e discretizzazione del problema usata nelle analisi FE.

critical slip surface. In the computation, the slip surfaces are assumed circular; the centre of the circular slip surface is shown with a point in the graph along with the corresponding value of *FS*. From the figure it can be observed that the slope is stable also at the end of the rainfall, with a value of $FS \geq 1$.

Figure 14 shows the pore water pressure isolines and the water table position in the case of rainfall event characterized by I = 60 mm/h at a time t = 2770 s – corresponding to the failure time observed during the laboratory test. Figure 15 shows the results of the stability analyses performed at the same time (t = 2770 s). In this case, the safety coefficient FS = 0.939 indicates the slope is not stable, according to the experimental evidences.

The results of the FE numerical analyses with the two considered rainfall rates show the different effect that the flow regime has on the slope stability. In the case of the lower rainfall rate (I = 15 mm/h), the response of the slope has been evaluated at the end of the seepage analysis and it can be observed that a rain infiltration process is still ongoing. The slope is still partially unsaturated in the upper part, resulting in stable condition. In the case of heavy rainfall rate (I = 60 mm/h), the slope response has been evaluated at the instant of collapse (about 45 minutes after the onset of rain) and it was observed that the slope is completely saturated, with a piezometric line at the ground surface, resulting in the overcoming of the limit equilibrium conditions, bringing up to failure.

5.2. Case of vegetated soil

As well known, the presence of roots increases the soil effective cohesion with no significant change in its friction angle (see, *e.g.*, WU *et al.*, 1979; 2013). Such mechanical effect can be introduced in the Mohr-Coulomb failure law through an "apparent cohesion" term, which adds to the soil effective cohesion (see, *e.g.*, WU *et al.*, 2015). The contribution of root reinforcement to the soil shear strength has been investigated in slope stability analyses, modifying the soil properties of the upper layer of the slope including vegetation. This approach allowed quantifying the effect of the mechanical root reinforcement on the slope factor of

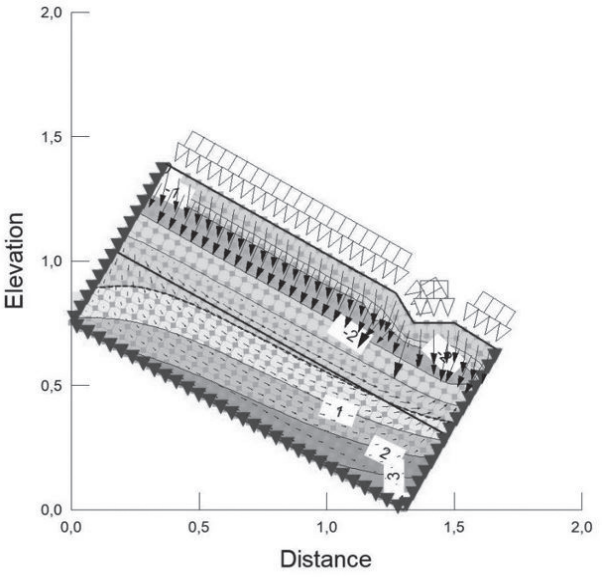

Fig. 12 – Isolines of pore water pressures at the end of the seepage analysis (for I=15 mm/h).
Fig. 12 – Isolinee della pressione interstiziale valutate al termine dell'analisi di filtrazione (con pioggia di intensità I=15 mm/h).

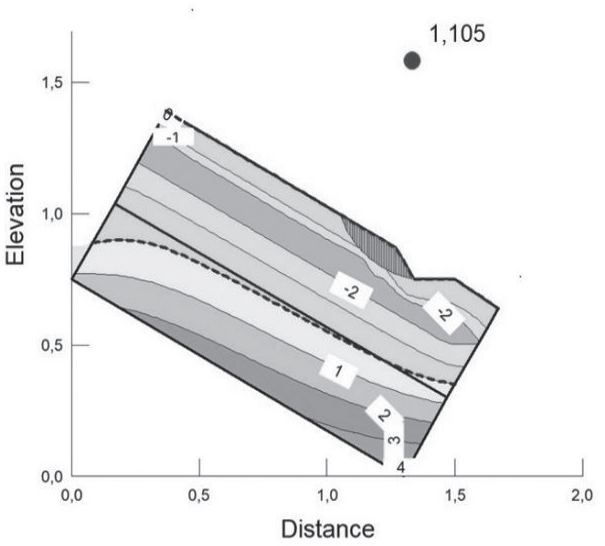

Fig. 13 – Slope stability analysis results at the end of the seepage analysis (for I=15 mm/h).
Fig. 13 – Risultati dell'analisi di stabilità eseguita al termine del processo di infiltrazione (con pioggia di intensità I=15 mm/h).

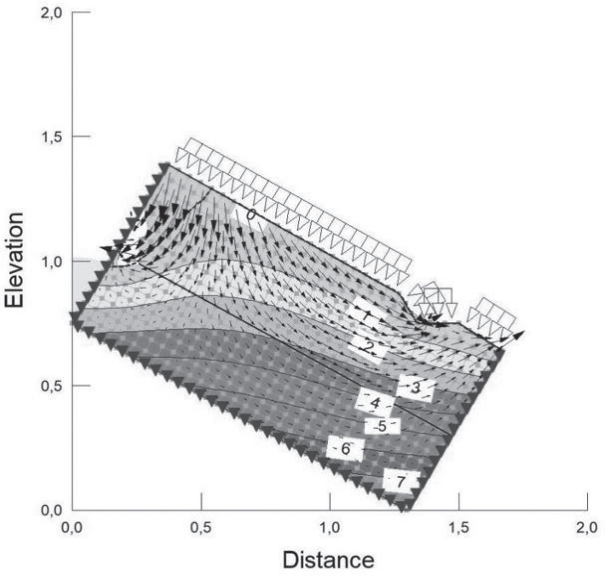

Fig. 14 – Isolines of the pore water pressures at t=2770 s during the transient seepage analysis (for I=60 mm/h).
Fig. 14 – Isolinee della pressione interstiziale valutate durante il transitorio di infiltrazione all'istante t =2770 s (i risultati sono relativi alla pioggia di intensità I=60 mm/h).

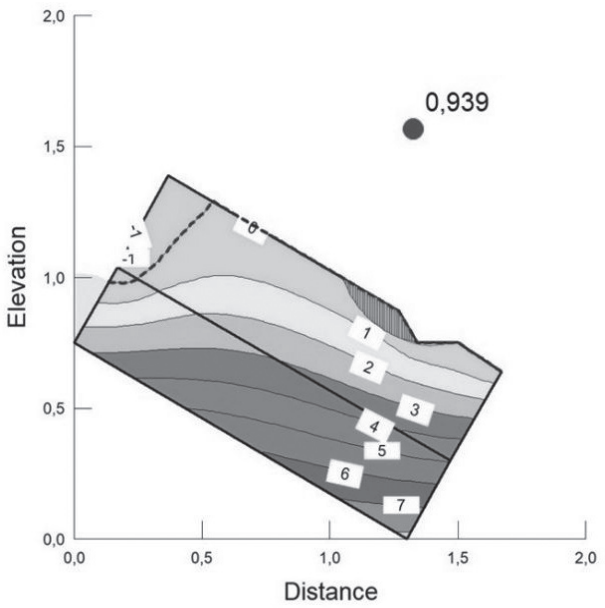

Fig. 15 – Slope stability analysis results at t=2770 s (for I=60 mm/h).
Fig. 15 – Risultati dell'analisi di stabilità all'istante t=2770 s del processo di infiltrazione (i risultati sono relativi alla pioggia di intensità I=60 mm/h).

safety and assessing the sensitivity of slope stability to the variation of apparent cohesion.

To this aim, the model presented in section 5.1 has been modified by introducing a shallow layer of 10 cm where the effect of the root is present. The numerical simulations performed in section 5.1 have been repeated to assess the minimum value of cohesion introduced by the grass root that brings the slope in stable condition, as observed in the experiments. The value was obtained through a back-analysis, imposing $FS = 1$. Figure 16 shows the results of the slope stability back-analysis carried out considering the presence of the vegetation on slope. The stability analysis has been performed for a rainfall event characterized by $I = 60$

mm/h and using the transient infiltration FEA results at the time t = 2770 s, which corresponds to the failure time observed in the laboratory test (the same seepage conditions of figure 15). To obtain a *FS* = 1, the results of the back-analysis indicated to adopt the following values for shear strength: =29° (as measured) and c'=10 kPa. Indeed, as shown in figure 16, an increasing of cohesion of 10 kPa is the assessed value able to bring the slope in stable conditions for the case-study considered. The obtained safety factor *FS* is 1.055, with an increment of 12% with respect to the FS of the bare slope. Numerical results are consistent with the experimental evidence showing vegetated slope is stable also during the most intense rainfall event. The estimated additional cohesive strength value is also in agreement with numerous literature references that suggest to account for the presence of vegetation as an additional contribution to strength with values of the same order of magnitude [NORRIS *et al.*, 2006; CECCONI *et al.*, 2012; SALCIARINI *et al.*, 2020b].

5.3. Combined effect of inclination and vegetation

For a more comprehensive investigation of the combined effect of inclination and vegetation on slope stability, the trend of the *FS* has been examined, under the effect of heavy rainfall conditions (I = 60 mm/h). The model described in section 5.1 and 5.2 was modified to reproduce the varying steepness conditions performed during the lab experiments (from 17° to 30°). Figure 17 summarizes at glance the results obtained for the complete set of simulations and figure 18 plots the predicted values of the *FS* at varying inclination and vegetation conditions.

The presence of a vegetated cover introduced in the model as an additional "apparent cohesion" described above produces a trend line that identifies safer conditions for the slope with respect to the bare slope (dashed line). The two lines of the graph have not a parallel trend and their gap increases for lower inclinations, meaning that the increasing of stability introduced by the roots tends to be more evident for lower steepness. This agrees with other results obtained by the Authors [SALCIARINI *et al.*, 2020b] where they demonstrated that countermeasures to increase the safety conditions of a slope based vegetations are more effective for mild inclinations. The decreasing values of *FS* with increasing inclination reach the limiting equilibrium conditions for the case of the bare slope (solid line), while they keep laying in the safe side of the graph (above the grey line, representing *FS* = 1) in presence of a vegetated cover.

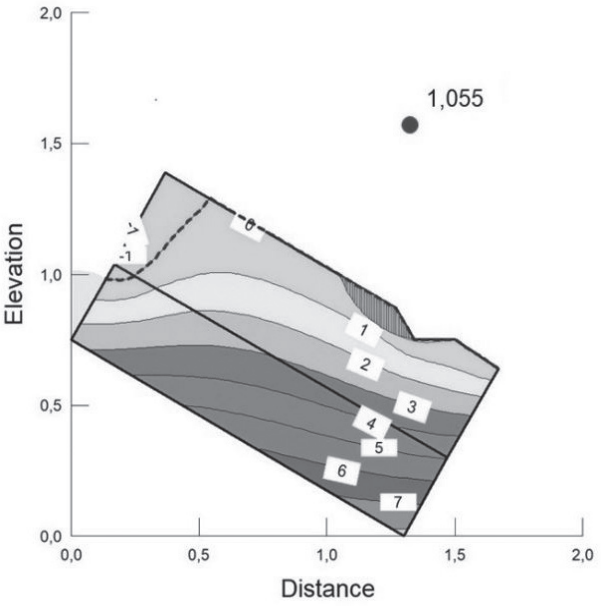

Fig. 16 – Slope stability analysis results at t=2770 s (I=60 mm/h), for vegetated soil 1 (adopting a cohesion of c'=10 kPa, and a friction angle of ϕ=29°).
Fig. 16 – Risultati dell'analisi di stabilità ottenuti all'istante t=2770 s del processo di infiltrazione nel caso di pendio vegetato (i risultati sono relativi alla pioggia di intensità I=60 mm/h, adottando per il terreno 1 una coesione c'=10 kPa, e un angolo di attrito ϕ=29°).

6. Conclusions

This paper describes laboratory experiments that were designed to investigate the response of slopes of different inclinations, hit by different rainfalls and with bare or vegetated surface. A small-scale model was constructed in laboratory, and the following observations were derived:

– the inclination of the saturated slope was progressively increased from 10° to 26°, applying the same rainfall conditions. At each inclination, the trend of the surface and deep outflow was monitored and the percentage of rainfall transformed into surface outflow was calculated. This set of experiments made it possible to observe that not only permeability but also the inclination of the topographical surface plays a role in the infiltration process, with an infiltration into the subsoil that decreases as the slope increases in an approximately linear manner.
– The slope was brought to the maximum inclination (30°) and an artificial excavation in the lower part was shaped. The other slope model characteristics were kept the same and it was subjected to different rainfalls, up to determining the one that leads it to failure conditions. Using a high-resolution camera, the evolution of the slope during the rainfalls was monitored

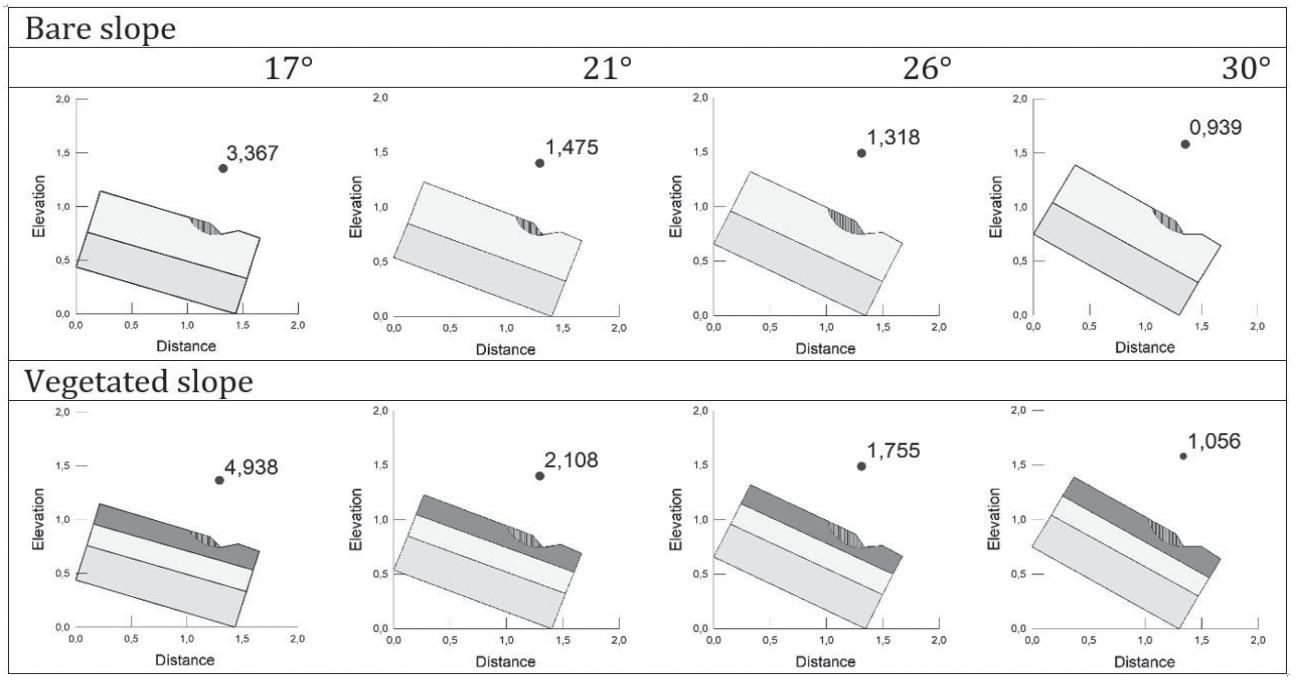

Fig. 17 – Summary of the complete set of simulations varying vegetation and inclination conditions.
Fig. 17 – Sintesi delle analisi effettuate al variare della pendenza nel caso di pendio denudato e vegetato.

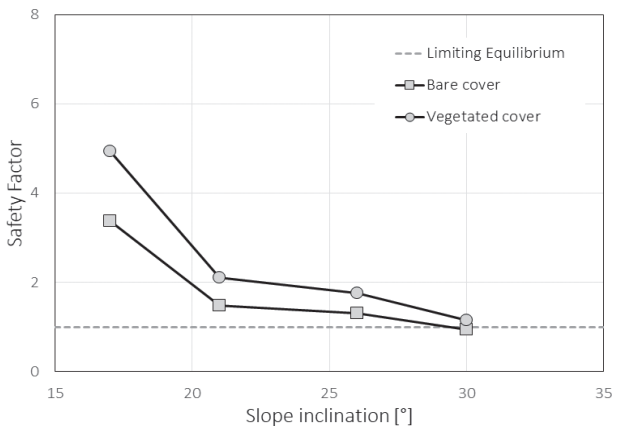

Fig. 18 – Trend of the safety factor FS at varying inclination and vegetation conditions.
Fig. 18 – Andamento del fattore di sicurezza FS in funzione dell'inclinazione del pendio e delle condizioni di assenza/presenza di vegetazione.

and the instant of the first failure was identified. After 45 minutes of rainfall, cracks appear in the upper part of the excavation until failure occurred.

– A grass carpet was sown on the surface of the slope, all the slope model characteristics were kept the same of the bare case and the slope model was subjected to the same intensity and duration of rainfall that had led to the failure of the bare slope. By the high-resolution camera, the evolution of the slope was monitored and the beneficial effect of the roots on the stability of the slope was qualitatively observed, with no evidences of rupture.

When SBE measures (like a grass carpet) are considered in slope stability, their effect needs to be quantified, *e.g.* in form of *FS* [WU *et al.*, 2015]. In doing so, some salient features of the soil-vegetation system should be considered and combined into a physically consistent model in order to model the complex interaction between soil, plant, water and atmosphere. In a simplified manner, for practical design purposes, simple infiltration models and analyses based on the limit equilibrium methods can be used to account for reinforcement by roots. In this work the enhancement of strength by plant roots has been considered as an additional cohesion, which is introduced into the Mohr-Coulomb failure criterion, as widely used by many Authors (see, *e.g.*, WU *et al.*, 2015). A 2D numerical model was prepared and a slope stability analysis was performed to assess the improvement of the soil properties due to the root.

First, the stability analysis of the bare slope was carried out, calibrating the numerical model on the experimental observations. In particular, the numerical model was set to reproduce the failure process monitored in the laboratory model, at the instant of the recorded time. Thus, the stability analysis was carried out after 45 minutes of rain, obtaining the values for the pore pressures at that time from a transient Finite Element infiltration analysis. Subsequently, the same numerical model was used to ob-

tain an estimate of the increase in resistance produced by the roots through back-analysis. The (minimum) value of the additional cohesion capable of producing the observed stability conditions was therefore estimated, equal to 10 kPa. This value is in the range of values proposed by numerous authors in the literature for SBE interventions based on grass carpet [CAZZUFFI *et al.*, 2006; NORRIS *et al.*, 2006; FLORINETH *et al.*, 2002; CALCATERRA *et al.*, 2004; PETRONE and PETRI, 2009; ZAROTTI *et al.*, 2014; SALCIARINI *et al.*, 2020b; SALCIARINI *et al.*, 2009].

A progress of this research will be investigating different combined effects on slope stability conditions, such as: depth of the root (related to vegetation growing stage), type of root architecture (related to specific species of vegetation), spatial layout of vegetation (related to pattern of the root system architecture). Also, coupling the current model with hydrogeological model to consider interconnected physical processes may improve the accuracy of the prediction.

In conclusion, despite some inherent limitations of the model presented in this work, results of the current study can give some insights to practitioners. The findings obtained in this research can be used as a guidance to enhance the confidence on the effectiveness of vegetation works in the stability of the slope.

Acknowledgment

This work has been carried out in the framework of the project PRIN2015: "Innovative monitoring and design strategies for sustainable landslide risk mitigation.".

References

BEVEN K.J. (2002) – *Rainfall-Runoff Modelling*. John Wiley & Sons, Chichester, UK; ISBN 978-0-470-71459-1.

BORDOLOI S., WAI NG C. W. (2020) – *The effects of vegetation traits and their stability functions in bio-engineered slopes: A perspective review*. Engineering Geology, 275, 105742.

CALCATERRA D., PALMA B., DORONZO G., DE LUCA TUPPUTI F. (2004) – *L'uso delle tecniche di Ingegneria Naturalistica nella mitigazione del rischio da frana: Alcuni esempi dalla Campania*. Quad. Geol. Appl. 11, n. 2.

CAMMERAAT E., BEEK R.V., KOOIJMAN A. (2005) – *Vegetation succession and its consequences for slope stability in SE Spain*. Plant and Soil, 278, pp. 135-147. doi:10.1007/s11104-005-5893-1

CASCINI L., CALVELLO M., GRIMALDI G.M. (2010) – *Groundwater modelling for the analysis of active slow moving landslides*. J. Geotech. Geoenviron. Eng Div, ASCE, 136, n. 9, pp. 1220-1230.

CASCINI L., CUOMO S., DELLA SALA M. (2011) – *Spatial and temporal occurrence of rainfall-induced shallow landslides of flow type: A case of Sarno-Quindici, Italy*. Geomorphology, 126, pp. 148-158.

CAZZUFFI D., CORNEO A., CRIPPA E. (2006) – *Slope stabilisation by perennial "gramineae" in Southern Italy: Plant growth and temporal performance*. Geotech. Geol. Eng., 24, pp. 429-447.

CECCONI M., PANE V., NAPOLI P., CATTONI E. (2012) – *Deep roots planting for surface slope protection*. Electron. J. Geotech. Eng., 17, pp. 2809-2820.

CORRADINI C., MORBIDELLI R., FLAMMINI A., GOVINDARAJU R.S. (2011) – *A parameterized model for local infiltration in two-layered soils with a more permeable upper layer*. J. Hydrol., 20, n. 396, pp. 221-232.

CORRADINI C., MELONE F., SMITH R.E. (1997) – *A unified model for infiltration and redistribution during complex rainfall patterns*. J. Hydrol., 192, pp. 104-124.

COTECCHIA F., PEDONE G., BOTTIGLIERI O., SANTALOIA F., VITONE C. (2014) – *Slope-atmosphere interaction in a tectonized clayey slope: a case study*. Rivista Italiana di Geotecnica.

FAY L., AKIN M., SHI X. (2012) – *Cost effective and sustainable road slope stabilization and erosion control*. National Academies of Sciences, Engineering and Medicine.

FENG S., LIU H.W., NG C.W.W. (2020) – *Analytical analysis of the mechanical and hydrological effects of vegetation on shallow slope stability*. Computers & Geotechnics, 118, 103335.

FLORINETH F., RAUCH H.P., STAFFLER H.P. (2002) – *Stabilization of landslides with bio-engineering measures in South Tyrol/Italy and Thankot/Nepal*. In: INTERPRAEVENT 2002 in the Pacific Rim, 2002, Matsumoto/Japan; Congress publication, vol. II, p. 827-837, Matsumoto/Japan.

GARIANO S.L., MELILLO M., PERUCCACCI S., BRUNETTI M.T. (2020) – *How much does the rainfall temporal resolution affect rainfall thresholds for landslide triggering?* Natural Hazards, 100, pp. 655-670 https://doi.org/10.1007/s11069-019-03830-x

GEO-SLOPE *International Ltd. Stability Modeling with GeoStudio*; GEO-SLOPE International Ltd., Calgary, AB, Canada, 2019.

HAQUE U., DA SILVA P.F., DEVOLI G., PILZ J., ZHAO B., KHALOUA A., WILOPO W., ANDERSEN P., LU P., LEE J., YAMAMOTO T., KEELLINGS D., WU J.H., GLASS G.E. (2019) – *The human cost of global warming: deadly landslides and their triggers (1995–2014)*. Sci Tot Environ, 682, pp. 673-684. https://doi.org/10.1016/j.scito tenv.2019.03.415

KHALILZAD M., GABR M.A., HYNES M.E. (2014) – *Effects of woody vegetation on seepage-induced deformation and related limit state analysis of levees*. Int. J. Geomechanics, 14, n. 2, pp. 302-12.

LAMMERANNER W., RAUCH H.P., LAAHA G. (2005) – *Implementation and Monitoring of Soil Bioengineering*

Measures at a Landslide in the Middle Mountains of Nepal. Plant Soil, 278, pp. 159-170.

LIU H.W., FENG S., NG CWW. (2016) – *Analytical analysis of hydraulic effect of vegetation on shallow slope stability with different root architectures*. Computers & Geotechnics, 80, pp. 115-20.

MORBIDELLI R., SALTALIPPI C., FLAMMINI A., CIFRODELLI M., CORRADINI C., GOVINDARAJU R.S. (2015) – *Infiltration on sloping surfaces: Laboratory experimental evidence and implications for infiltration modelling*. J. Hydrol., 523, pp. 79-85.

MORBIDELLI R., SALTALIPPI C., FLAMMINI A., GOVINDARAJU R.S. (2018) – *Role of slope on infiltration: A review*. J. Hydrol., 557, pp. 878-886.

MORBIDELLI R., CORRADINI C., SALTALIPPI C., FLAMMINI A., DARI J., GOVINDARAJU R. S. (2019) – *A New Conceptual Model for Slope-Infiltration*. Water.

MORGAN R.P., RICKSON R.J. (2003) – *Slope Stabilization and Erosion Control: A Bioengineering Approach*. Taylor & Francis: Abingdon, UK.

MORGENSTERN N. R., PRICE V. E. (1965) – *The Analysis of the Stability of General Slip Surfaces*. Géotechnique, 15, n. 1, pp. 79-93. Doi-10.1680/geot.1965.15.1.79

NORRIS J., GREENWOOD J.R. (2006) – *Assessing the role of vegetation on soil slopes in urban areas*. In: Proceedings of the 10th IAEG International Congress, Nottingham, UK, 6-10 September 2006.

OPERSTEIN V., FRYDMAN, S. (2000) – *The influence of vegetation on soil strength*. Proc. Inst. Civ.-Eng.-Ground Improv., 4, pp. 81-89.

PETRONE A., PRETI F. (2009) – *Soil bio-engineering for risk mitigation and environmental restoration in a humid tropical area*. Hydrology & Earth System Sciences Discussions,, 6, n. 4, pp. 5139-5176.

PICARELLI L. (2007) – *Considerations about the mechanics of slow active landslides in clay*. In: Progress in Landslide Science; K. Sassa, H. Fukuoka, F. Wang, G. Wang (Eds.), Springer: Berlin, Germany, 2007, pp. 27-57.

ROTISCIANI G.M., DESIDERI A., AMOROSI A. (2021) – *Unsaturated structured soils: constitutive modelling and stability analyses*. Acta Geotechnica, https://doi.org/10.1007/s11440-021-01313-7

ROTISCIANI G.M., LALICATA L.M., DESIDERI A., CASINI F. (2020) – *Numerical modelling of the response of an unsaturated silty soil under wetting and gravitational loading processes*. In: E3S Web of Conferences Open Access Volume CXCV, 16 October 2020, Article number 02012, 4th European Conference on Unsaturated Soils, E-UNSAT 2020, Lisboa, 19 October 2020 – 21 October 2020.

SALCIARINI D., VOLPE E., KELLEY S.A., BROCCA L., CAMICI S., FANELL I G., TAMAGNINI C. (2015) – *Modeling the effects induced by the expected climatic trends on landslide activity at large scale*. Procedia Engineering, 158, pp. 541-545.

SALCIARINI D., TAMAGNINI C., RONCHI F., VOLPE E., FANELLI G. (2017) – *An approach for large-scale soil characterization for the application of non-structural landslide risk mitigation*. Rivista Italiana di Geotecnica, 51, n. 3, pp. 7-21.

SALCIARINI D., BROCCA L., CAMICI S., CIABATTA L., VOLPE E., MASSINI R., TAMAGNINI C. (2019) – *Physically based approach for rainfall-induced landslide projections in a changing climate*. Proceedings of the Institution of Civil Engineers, Geotechnical Engineering, 172, n. 6, pp. 481-495.

SALCIARINI D., VOLPE E., CATTONI E. (2020) – *Probabilistic vs. deterministic approach in landslide triggering prediction at large–scale*. Lecture Notes in Civil Engineering, 40, pp. 62-70.

SALCIARINI D., VOLPE E., DI PIETRO L., CATTONI E. (2020b) – *A Case-Study of Sustainable Countermeasures against Shallow Landslides in Central Italy*. Geosciences 10, n. 4, p. 130. https://www.mdpi.com/2076-3263/10/4/130.

SALCIARINI D., TAMAGNINI C., CONVERSINI P. (2009) – *Numerical approaches for rockfell analysis: a comparison*. In: 18th World IMACS Congress and MODISM 2009, Cairns 13-17 July 2009, pp. 2706-2716.

VOLPE E., CIABATTA L., SALCIARINI D., CAMICI S., CATTONI E., BROCCA L. (2021) – *The Impact of Probability Density Functions Assessment on Model Performance for Slope Stability Analysis*. Geosciences 11, n. 8, pp. 322. https://doi.org/10.3390/geosciences11080322

SMITH R.E., PARLANGE, J.-Y. (1978) – *A parameter-efficient hydrologic infiltration model*. Water Resources Resarch, 14, pp. 533-538.

STOKES A., ATGER C., BENGOUGH A.G., FOURCAUD T., SIDLE R.C. (2009) – *Desirable plant root traits for protecting natural and engineered slopes against landslides*. Plant Soil 2009, 324, pp. 1-30.

WALDRON L. (1977) – *The shear resistance of root-permeated homogeneous and stratified soil*. Soil Sci. Soc. Am. J., 41, pp. 843-849.

WU T.H., MCKINNELL III, W.P., SWANSTON D.N. (1979) – *Strength of tree roots and landslides on Prince of Wales Island, Alaska*. Canadian Geotechnical Journal, 16, pp. 19-33.

WU T.H. (2013) – *Root reinforcement of soil: review of analytical models, test results, and applications to design*. Canadian Geotechnical Journal, 50, pp. 259-274.

WU W., SWITALA B.M., TAMAGNINI R., AURER M., GRAF F., TE KAMP L., XIANG W. (2015) – *Effect of Vegetation on Stability of Soil Slopes: Numerical Aspect*. In: W. Wu (Eds.) Recent Advances in Modeling Landslides and Debris Flows. Springer Series in Geomechanics and Geoengineering. Springer, Cham. https://doi.org/10.1007/978-3-319-11053-0_15

ZAYADI R., KUSUMA Z., LEKSONO A. S., YANUWIADI B. (2020) – *The influence of vegetation roots on slope stability in landslide susceptible areas*. International Journal of Civil Engineering and Technology (IJCIET), 11, n. 4, pp. 124-133.

ZAROTTI C. (2014) – *L'interazione pendio atmosfera:*

piante erbacee a radicazione profonda per la protezione dei versanti in caso di fenomeni meteorologici intensi. In: Proceedings of the XXV Convegno Nazionale di Geotecnica: la geotecnica nella difesa del territorio e delle infrastrutture dalle calamità naturali, Baveno, Italy, June 2014.

Modellazione fisica e numerica della risposta di un pendio sottoposto a diverse condizioni di pioggia, inclinazione e vegetazione

Sommario

In questa memoria vengono presentati i risultati di uno studio sperimentale e numerico condotto per quantificare l'effetto di diversi fattori cruciali nell'evoluzione dei versanti, quali: la pioggia, l'inclinazione della superficie topografica e la presenza di vegetazione. È stata esaminata la risposta di un pendio a scala ridotta realizzato in laboratorio variando le seguenti condizioni: a) pendenza, attraverso un sistema di pistoni idraulici; b) caratteristiche della pioggia (in termini di intensità e durata), attraverso un simulatore di pioggia artificiale; c) presenza/assenza di una copertura vegetale. La prima serie di prove ha consentito di definire un andamento della percentuale di infiltrazione di pioggia all'interno del modello di pendio in funzione della sua pendenza. La seconda serie di prove ha consentito di osservare il comportamento del pendio a rottura nelle condizioni di assenza di vegetazione; infine, il terzo set ha dimostrato l'effetto benefico di un manto erboso sulla stabilità del pendio. Tutti gli esperimenti di laboratorio sono stati riprodotti attraverso simulazioni numeriche, utilizzando il codice SEEP/w FE per le analisi di infiltrazione in regime transitorio e il codice SLOPE/w per le analisi di stabilità. Le analisi a ritroso, basate sui metodi classici dell'equilibrio limite, hanno consentito di stimare il contributo incrementale alla resistenza al taglio del terreno fornito dalla presenza delle radici, rilevante nelle applicazioni pratiche per interventi di consolidamento basati su tecniche di ingegneria naturalistica.